JOURNAL OF AGRICULTURAL AND FOOD CHEMISTRY

Gene Isolation, Analysis of Expression, and in Vitro Synthesis of Glutathione *S*-Transferase from Orange Fruit [*Citrus sinensis* L. (Osbeck)]

ANGELA ROBERTA LO PIERO, IVANA PUGLISI, AND GOFFREDO PETRONE*

Dipartimento di Scienze Agronomiche, Agrochimiche e delle Produzioni Animali (DACPA), Facoltà di Agraria, Università degli Studi Catania, via S. Sofia no. 98, 95123 Catania, Italy

Glutathione *S*-transferases (*GST*s) (EC 2.5.1.18) are ubiquitous enzymes that have a defined role in xenobiotic detoxification, but a deeper knowledge of their function in endogenous metabolism is still lacking. In this work, we isolated the cDNAs as well as the genomic clones of orange *GST*s. Having considered gene organization and homology data, we suggest that the isolated *GST* gene is probably involved in the vacuolar import of anthocyanins. We also found that the blood and blond orange *GST*s shared the same nucleotide sequences, but as expected, the *GST* expression in the nonpigmented orange cultivar [*Citrus sinensis* L. (Osbeck)] (Navel and Ovale) was strongly reduced as compared to that of the pigmented orange (Tarocco). Interestingly, in the crude extracts of pigmented orange fruits, the *GST* activity was reproducibly detected by providing either 1-chloro-2,4 dinitrobenzene (CDNB) or cyanidin-3-*O*-glucoside (C-3-G) as substrates; moreover, we have shown that cyanidin-3-*O*-glucoside acted as a powerful competitive inhibitor of 1-chloro-2,4 dinitrobenzene conjugation to reduced glutathione (*GSH*) in the pigmented orange, confirming that this molecule might easily bind to the active site of the enzyme and functions as a putative substrate. In addition, we have reported here the successful in vitro expression of orange *GST* cDNAs leading to a *GST* enzyme that is active against cyanidin-3-*O*-glucoside, thus suggesting the probable involvement of the isolated gene in the tagging of anthocyanins for vacuolar import. This last result will help to study the kinetic and structural properties of orange fruit *GST* avoiding time-consuming protein purification procedures.

KEYWORDS: Anthocyanin; blood oranges; *Citrus sinensis*; cold stress; glutathione *S*-transferase; real-time PCR

1. INTRODUCTION

Glutathione *S*-transferases (*GST*s) are a family of dimeric enzymes whose primary function is to catalyze the nucleophilic attack of the tripeptide glutathione (γ-L-glutamyl-L-cysteinyl-L-glycine) on lipophilic cosubstrates with a reactive electrophilic center, thus forming a polar S-glutathionylated conjugate (*1*). This is considered to be a crucial step in the detoxification process of xenobiotic molecules because the S-glutathionylated metabolites produced are either further catabolized and excreted in animals or tagged for vacuolar import because of the lack of effective excretion pathways in plants (*2*). In plants, glutathione conjugates are substrates for ATP-driven export pumps (GS-X) located in the tonoplast that can sequester structurally diverse glutathione-tagged compounds into the vacuole (*3*−*6*). Individual *GST*s are differentially regulated in response to many forms of biotic and abiotic stress, suggesting diverse functions in endogenous metabolism. Thus, specific *GST*s are reported to be induced upon infection, in response to treatment with ozone, plant hormones, heavy metals, heat shock, dehydration, wounding, and senescence (*1*).

Despite their well-known role in stress physiology, as well as in acute detoxification of applied chemicals, a deeper insight into matching specific *GST* isozymes with either their preferred substrates or their function in vivo in normal cellular processes has not yet been achieved. Presently, glutathione conjugates to endogenous secondary plant products, especially derivatives of the phenylpropanoid pathway such as cinnamic acids or anthocyanins, are reported (*1*). The biosynthesis of anthocyanins occurs in the cytosol, but neither these pigments nor their intermediates have been detected there, and only the end product, the anthocyanins, but not their intermediate, are detected in the vacuoles, where stable anthocyanin pigmentation occurs (*7*). In maize, it has been shown that the last genetically defined step of anthocyanin biosynthesis is encoded by *bronze2* (*8*). The gene product *BZ2* showed high homology with glutathione *S*-transferases and was able to transfer glutathione to the artificial substrates 1-chloro-2,4-dinitrobenzene (CDNB) (*8*). In the

* Author to whom correspondence should be addressed. Phone: 0039-(0)95-7580239. Fax: 0039-(0)95-7141581. E-mail: goffredo.petrone@unict.it.

10.1021/jf0616816 CCC: $33.50
Published on Web 10/28/2006

presence of a functional *bronze2* (*BZ2*), anthocyanins accumulate within the vacuoles, whereas when the *bronze2* gene is missing, anthocyanins were found retained in the cytosol, thus conferring to the kernels a pale brown phenotype due to pigment oxidation (*8*). These oxidized secondary metabolites in the cytoplasm of *BZ2* mutants are somewhat toxic, diminishing the overall vigor of the plant (*9*). Therefore, it was supposed that glutathionation of anthocyanins is a prerequisite for vacuolar import because GS conjugates are reported to be very efficient substrates of an ATP-driven ABC transporter (*6*). Subsequent studies (*10*) showed that the *anthocyanin9* gene (*AN9*) involved in the anthocyanin biosynthesis in petunia also shares high homology with glutathione transferases and that *BZ2* and *AN9* can functionally complement each other in maize and petunia, respectively, even though these genes are highly divergent as they belong to different subfamilies of glutathione transferases (*10*). More recently, novel *Arabidopsis* mutants, *transparent testa 19* (*TT19*), showed a great reduction of anthocyanins in the vegetative parts as well as brown pigments in the seed coat (*11*). The *TT19* gene was isolated, and it was shown to be a member of the *Arabidopsis* glutathione *S*-transferase gene family. Heterologous expression of the putative ortholog *AN9* in *TT19* mutants complemented the lack of anthocyanin accumulation, suggesting that the *TT19* gene is required for vacuolar uptake of anthocyanins (*11*). However, based on their studies, Mueller et al. (*12*) suggested that *BZ2* and *AN9* act as flavonoid binding proteins during the transfer of anthocyanins into the vacuole without forming a glutathionylated adduct, although it has been shown that yet another secondary compound, the phytoalexin medicarpin, is transported into vacuoles as a glutathione conjugate (*13*).

Several selected sweet orange [*Citrus sinensis* (L.) Osbeck] cultivars, such as Tarocco, Moro, and Sanguinello (blood cultivars) are characterized by the presence, in both flesh and rind, of anthocyanins, which are absent in the blond orange cultivars such as Navel, Ovale, and Valencia (*14*). Among the anthocyanins, cyanidin-3-*O*-glucoside represents 97% of the total pigment content (*15*), thus giving orange fruits distinctive antioxidant properties because of its very negative redox potential ($E_{1/2} = -405$ mV) (*16*). We previously isolated partial cDNA clones of six enzymes active in the later steps of the anthocyanin biosynthetic pathway, chalcone synthase (CHS), chalcone isomerase (CHI), flavonol 3′hydroxylase (F3′H), dihydroflavonol 4-reductase (DFR), anthocyanidin synthase (ANS), and UDP-glucose flavonoid glucosyl transferase (UFGT) from *Citrus sinensis* L. Osbeck (*17*), and showed by quantitative real-time PCR that transcripts encoding the late enzymes such as DFR, ANS, and UFGT are significantly reduced in non-red oranges as compared to red cultivars (*18*−*20*). Moreover, the impact of a low-temperature exposure (4 °C) on both anthocyanin production and expression of some of the structural genes involved in the biosynthesis of these pigments [phenylalanine ammonia lyase (*PAL*), *CHS*, *DFR*, and *UFGT*] was also investigated (*21*). Our results showed that the anthocyanin content of fruits exposed to low temperature dramatically increased throughout the storage period in contrast to the pigment levels reached in orange fruits kept at room temperature (25 °C). The accumulation of anthocyanins induced by low-temperature storage was accomplished by a 40-fold increase in the *PAL*, *CHS*, *DFR*, and *UFGT* transcripts, thus suggesting that the genes involved in anthocyanin biosynthesis have to be considered as *cor* (cold regulated) genes (*21*).

The aim of this work was to isolate and characterize a *GST* gene putatively involved in *GSH* tagging of anthocyanins in orange fruits, as we assumed that this enzyme might represent the last step of the anthocyanin biosynthesis in orange fruits as described in maize (*8*) and petunia (*10*). We presented the results obtained on the differential expression of the cloned *GST* gene in the juice vesicles of both blood and blond oranges monitored by quantitative real-time PCR. To evaluate the kinetic properties of the enzyme, we also assayed the *GST* activity in the red orange extracts. Moreover, the effect of low-temperature storage on the expression of blood orange *GST* was also monitored to determine whether the transcription of the orange fruit *GST* is enhanced by this treatment. Finally, an active *GST* from orange cDNA was also expressed in a cell-free system, this being the first report of an in vitro expression of *GST* from fruit tissues.

2. MATERIALS AND METHODS

2.1. Plant Material. Pigmented (Tarocco) and nonpigmented (Navel and Ovale) oranges [*C. sinensis* (L.) Osbeck] were harvested at commercial maturity from approximately 15 year-old trees grown at a private farm in the territory of Francofonte, Italy. Freshly harvested orange fruits were peeled, chopped into 1 g samples, immediately frozen with liquid nitrogen, and stored at −80 °C until use.

2.2. Extraction of Genomic DNA and Total RNA. Genomic DNA from orange fruit juice vesicles was extracted using Plant DNAzol as extracting solution, whereas TriZol was employed to extract total RNA. DNA and RNA were routinely quantified using the DNA and RNA Quant-it assay kits, respectively. The nucleic acid extracting solutions and the DNA and RNA Quant-it assay kits were all obtained from Invitrogen (Carlsbad, CA).

2.3. cDNA Synthesis and Isolation of Orange Fruit *GST* Partial Clone. Reverse transcription was achieved by using 2 μg of total RNA from Tarocco and Navel orange fruit juice vesicles and the Superscript RNAse H⁻ First-strand synthesis kit (Invitrogen, Carlsbad, CA). To isolate the *GST* cDNA partial clone, two oligonucleotides designed on the basis of conserved nucleotide sequences of *Petunia hybrida* and *A. thaliana GST*s were used: forward primer (5′AAAATGGT(GT)GT-(CG)AAAGT(AG)(CT)ATGG3′) and reverse primer (5′TCAACTTC-(CT)A(CG)CCA(CT)TG(GA)TC3′). The PCR reaction was carried out using the following conditions: 95 °C × 1 min (1 cycle), 95 °C × 40 s, 55 °C × 40 s, 72 °C × 1 min (35 cycles), and 72 °C × 5 min (1 cycle). The PCR experiment produced an amplification product of 500 bp, whose identity was confirmed by sequencing.

2.4. Isolation of Genomic and cDNA *GST* Clones. On the basis of the specific sweet orange *GST* sequence obtained from the previously described PCR experiment, several steps of a genome walker and of 3′ RACE were performed to isolate both the 5′ and the 3′ DNA ends of the *GST* gene from blond (Navel) and blood (Tarocco) orange juice vesicles. Then, forward and reverse primers bordering the *GST* gene were designed, (*GST* for-5′ATGGTTGTTAAAGTGTATGGT-TCAGTT3′) and (*GST* rev-5′TTAATGAGCAAGACTCGCTAG-TTTC3′), and used in the following PCR strategies: (A) cDNA as template (200 ng): 94 °C × 5 min (1 cycle), 94 °C × 30 s, 55 °C × 30 s, 72 °C × 1 min (30 cycles), and 72 °C × 20 min (1 cycle); (B) genomic DNA (200 ng) as template: 94 ° × 5 min (1 cycle), 94 °C × 45 s, 55 °C × 30 s, 72 °C × 2 min (30 cycles), and 72 °C × 20 min (1 cycle). Accuprime *Pfx* DNA polymerase (Invitrogen, Carlsbad, CA) was used to isolate the orange *GST* cDNA and *GST* genomic clones from pigmented (Tarocco) and nonpigmented (Navel) oranges. The PCR products were purified, cloned into the PCR4-TOPO vector, and sequenced. Experiments were repeated at least three times on independently isolated nucleic acid preparations to discriminate authentic sequence mutations from procedure-linked mistakes.

2.5. Measurement of *GST* Expression by Real-Time Quantitative PCR. Real-time PCR, Taqman assays, were performed using the SuperScript III Platinum two-step qRT-PCR kit (Invitrogen, Carlsbad, CA) in a Smart Cycler II PCR machine (Cepheid). Pure mRNA was prepared from freshly harvested juice vesicles using the Quickprep mRNA purification kit (Amersham). Reverse transcription of mRNA (500 ng) was achieved by following the manufacturer's protocol. Primers and probe were as follows: for-Citrus-*GST* (5′GCAGCAAAG-

TATGCAAACC3′), rev-Citrus-*GST* (5′GAGCCATTGATCCAC-CAAAG'3′), and *GST*-probe (5′FAM-CCAAACCTACTTGGAAA-CACACTAGAAGAG-3′TAMRA). The relative quantitation of *GST* expression between blood and blond oranges was calculated using the comparative threshold (C_T) method (*22*). Three independent triplicates of quantitative PCR experiments were performed for each gene to generate an average C_T and to calculate standard deviation. The housekeeping gene elongation factor (EF), which has been reported to be constitutively expressed (*23*), was used as an endogenous reference, and ΔC_T was calculated by subtracting the average *EF-1*α C_T from the average C_T of the gene of interest. This value was calculated for each sample (Tarocco, Navel, and Ovale cDNA), and then the comparative expression level of the *GST* genes was given by the formula $2^{-\Delta\Delta C_T}$, where $-\Delta\Delta C_T$ was calculated by subtracting the baseline's ΔC_T from the sample's ΔC_T, where the baseline represents the minimum level of expression (Navel). The dynamic range of both *GST* and *EF-1*α was determined by monitoring the variation of ΔC_T with template dilution; the efficiency was very similar for both primer/probe systems. Elongation factor forward and reverse primers were as follows: for-Citrus-EF (5′CACCACCCCCAAGTACTC3′), rev-Citrus-EF (5′GT-TGTCACCCTCGAAACC3′), and EF-probe (5′FAM-AAGGTTG-GATACAACCCCGAGAAAGTCCCA3′-TAMRA). For each triplicate, 5 ng of cDNA was added to a final volume of 25 μL with a final concentration of 1X Platinum two-step qRT-PCR master mix (Invitrogen, Carlsbad, CA), 100 nM each primer, and 100 nM probe. Negative controls without reverse transcriptase were routinely included. Experiments were repeated at least three times on independently isolated mRNA preparation.

2.6. Enzyme Extraction. Freshly harvested red orange fruits (Tarocco) were peeled, chopped into small pieces, and homogenized using a waring blender with extraction buffer (0.1 M Tris-HCl pH 8.8 containing 0.4 M NaCl, 10% glycerol, 20 mM sodium ascorbate, 2.5% polyvinylpyrrolidone) in a 1:2 w/v ratio. The homogenate was filtered through two layers of cheesecloth and centrifuged at 10 000*g* × 10 min to remove solid particles. The pellet was discarded, whereas the supernatant was further centrifuged at 150000*g* × 30 min. Proteins of the soluble fraction were precipitated by 70% saturated ammonium sulfate, collected by centrifugation (12000*g* × 30 min), and resuspended in 1.5 mL of extraction buffer. The sample was then desalted by dialysis against a total of two 4 L extraction buffer changes for 10 h. All procedures were carried out at 4 °C. The protein concentration was determined according to the method of Bradford (*24*) using bovine serum albumin as a standard. The *GST* activity on crude extract of red orange fruit was assayed as described next. The experiments were repeated four times on independently prepared crude extracts.

2.7. In Vitro Expression of *GST*. The *GST* gene was PCR-amplified from a TOPO-plasmid *GST* clone with the Accuprime *Pfx* DNA polymerase PCR kit. The primers (forward, 5′CACCATGGTTGT-TAAAGTGTATGGTTCAGTT 3′, introducing the 5′ underlined CACC tail suitable for directionally cloning in pENTR-TOPO vector, and reverse, 5′ TTAATGAGCAAGACTCGCTAGTTTC3′) were used in a PCR experiment performed according to the manufacturer's instructions. The PCR product was purified and cloned into the TOPO-pENTR vector; once the ligation reaction was performed, the TOPO-pENTR-*GST* construct was used to transform into *Escherichia coli* One Shot TOP10 chemically competent cells. Positive clones were identified both by PCR analysis of the insert and by sequencing with M13 forward and reverse primers. The *GST* coding sequence was then transferred from the entry construct (pENTR-*GST*) into the pEXP1-DEST Gateway vector using the Gateway LR Clonase Enzyme mix based on the site-specific recombination properties of bacteriophage lambda. After the recombination reaction, the *GST*-pEXP1-DEST was used to transform into *E. coli* library efficiency DB3.1 competent cells. The presence and identity of the insert was tested both by PCR analysis and by sequencing with the T7 promoter and T7 reverse primers. In vitro expression of functionally active *GST* was achieved by using the cell-free protein system Expressway Plus by incubating the plasmid (*GST*-pEXP1-DEST) in the IVPS Plus *E. coli* extract for 4 h at 25 °C to promote proper protein folding. A negative control was also performed by incubating the *E. coli* extract with empty plasmid (pEXP1-DEST). The TOPO-pENTR vector, the pEXP1-DEST Gateway vector, the Gateway LR Clonase Enzyme mix, and the cell-free protein system Expressway Plus were all obtained from Invitrogen (Carlsbad, CA).

2.8. *GST* Enzyme Assays. The *GST* assay was performed by slightly modifying the method described in Holt et al. (*25*). The reaction mixture (final volume 0.5 mL) containing 1X PBS pH 7.4, 1 mM glutathione, 1 mM CDNB, or 1 mM NPE and enzyme extract (10−30 μg) was incubated at 30 °C for 15 min. GS-DNB conjugates were detected by measuring the absorbance of samples at 340 nm. All measurements were adjusted by subtracting the absorbance values obtained for the nonenzymatic conjugation of substrates. Molar extinction coefficients of 9600 M^{-1} cm^{-1} (CDNB) and 1200 M^{-1} cm^{-1} (NPE) were used. Steady-state analysis measurements of blood orange *GST* were performed in the presence of 1.5 mM GSH, whereas CDNB was used in the concentration range of 0.05−1.5 mM. The apparent kinetic parameters k_{cat} and K_m were determined by first fitting the collected steady-state data to the Michaelis−Menten equation to monitor that the CDNB concentrations were sufficient to gain enzyme saturation, and subsequently, data were analyzed in a double reciprocal plot. To test the effect of C-3-G on apparent kinetic parameters of the enzyme, initial velocities were contextually measured in the presence of 80 μM C-3-G. All initial velocities were determined in triplicate in buffers equilibrated at constant temperature. Moreover, to determine *GST* activity against C-3-G, the concentration of the remaining free thiol group of nonconjugated GSH was measured using a 5 mM solution of the Ellman reagent (5,5′-dithio-bis (2-nitrobenzoic acid) prepared in 0.1 M phosphate buffer pH 7.2 containing 0.1 mM EDTA. The reaction was carried out in a final volume of 0.25 mL containing 0.1 M phosphate buffer pH 6.8, 1 mM GSH, and 1 mM substrates (C-3-G, CNBD, or NPE) and incubated at 30 °C for 15 min. The free thiol concentration was assayed by adding to each sample an equal volume of the Ellman reagent (2 mL) and by measuring the absorbance at 412 nm immediately after the addition of the reagent. All measurements were adjusted by subtracting the decrease of free thiol groups due to oxidation of GSH to GS-SG. This was achieved by performing a sample blank in which the reaction mixture was incubated in the absence of the enzyme, which was added immediately after the Ellman reagent. A standard curve was prepared using GSH in a concentration range between 0 and 1.2 mM.

2.9. Cold Induction Experiment. Pigmented oranges (Tarocco) [*C. sinensis* (L.) Osbeck] were harvested in January 2004 from approximately 15-year-old trees grown at a private farm in the territory of Francofonte, Italy. Freshly harvested oranges were washed with distilled water, gently dried with paper towels, and then left to dry at room temperature for 3 h. Subsequently, orange fruits were randomly placed in two boxes (150 fruits per box), one of which was stored in a ventilated cold room at 4 °C and 90−95% relative humidity (RH) (cold stored samples). The other box was placed in a temperature-controlled device kept at 25 °C and 90−95% relative humidity (RH) (control samples). Samplings were carried out before storage (time 0) and every 15 days for a total storage period of 75 days. During each sampling, 18 fruits per box were collected and divided into three subgroups of six fruits each. Orange fruits of each subgroup were then peeled, chopped, and mixed to constitute three independent mean samples; the orange flesh was then immediately frozen with liquid nitrogen and stored at −80 °C until use (*21*).

2.10. Total Anthocyanin Content. Anthocyanin determination was performed as described in ref *21*.

2.11. PCR Product Analysis, Cloning, and Sequencing. PCR products were separated by 1.1% agarose gel containing 0.5 μg/mL ethidium bromide. The Qiaquick gel extraction kit and the Qiaquick PCR purification kit, both purchased from Qiagen (Valencia, CA), were used to extract PCR fragments from the agarose gels and PCR amplification reaction mixture, respectively. The amplified fragments were cloned into vector PCR4 TOPO vector and sequenced by the fluorescence detection method using both T7 and T3 as primers. Primers, Taqman probes, and DNA sequences were obtained from MWG-Biotech (Ebersberg, Germany). Comparison of the deduced amino acid sequences was performed by using the multiple sequence alignment program CLUSTALW 1.8 (www.ebi.ac.uk/clustalw). The nucleotide sequences reported in this paper have been submitted to Genbank under accession numbers DQ207360 (Navel *GST* genomic

```
Citrus sinensis          (DQ198153)   1  MVVKVYGSVKAACPQRVLACLLEKGVEFEIVQVDLDEGEHKRPEFLLRQPFGQVPVIEDG 60
Vitis vinifera           (AY971515)   1  MVMKVYGPVRAACPQRVLACLVEKGVEFEVVHVDLDSGEQKRPDFLLRQPFGQVPVVEDG 60
Petunia x hybrida        (Y07721)     1  MVVKVHGSAMAACPQRVMVCLIELGVDFELIHVDLDSLEQKKPEFLVLQPFGQVPVIEDG 60
Arabidopsis thaliana     (AB005238)   1  MVVKLYGQVTAACPQRVLLCFLEKGIEFEIIHIDLDTFEQKKPEHLLRQPFGQVPAIEDG 60
Glycine max              (AF243377)   1  -----YG-PTYGSPKRVLVCLIEKEIEFETVHVDLFKGENKEPEFLKLQPFGSLPVIQDG 54
Phaseolus acutifolius    (AY099257)   1  MVLKVYG-PTCASTKRVLVCLLEKEVEFEVIPVDLTKGEHKDPEFLKLQPFGVVPVIQDG 59
                                           *         **  *  *    **    **   * * *  *  **** *   **

Citrus sinensis          (DQ198153)  61  DFKLFESRAIIRYYAAKYANQGPNLLGNTLEEKALVDQWLEVEAHNFNDLAFNLVLQLVI 120
Vitis vinifera           (AY971515)  61  DFRLFESRAIVRYIAAKYAEQGPDLLGKSLEEKAVVDQWLEVEAHNFNELVYTLVMQLVI 120
Petunia x hybrida        (Y07721)    61  DFRLFESRAIIRYYAAKYEVKGSKLTGTTLEEKALVDQWLEVESNNYNDLVYNMVLQLLV 120
Arabidopsis thaliana     (AB005238)  61  DFKLFESRAIARYYATKFADQGTNLLGKSLEHRAIVDQWADVETYYFNVLAQPLVINLII 120
Glycine max              (AF243377)  55  DYTLYESRAIIRYLAEKYKDQGTDLLGKTIEEKGLVEQWLEVEAHNFHPPLYNLVINVLF 114
Phaseolus acutifolius    (AY099257)  60  DYTLYESRAIMRFYADKFRSQGVELLGRTAEERGVVEQWLEVEAHNFHPPAYDLAVHVLF 119
                                           *  * ***** *  * *    *  * *   *    * **  **

Citrus sinensis          (DQ198153) 121  LPRMGQRSDTALVHNLEQKLEAVLNIYEQRLSKSNYLAGDSFTLADLSHLPALRYLMNEA 180
Vitis vinifera           (AY971515) 121  LPRMGERGDLALAHTCEQKLEKVFDVYEQRLSKSRYLAGDSFTLADLSHLPAIRYLVKEA 180
Petunia x hybrida        (Y07721)   121  FPKMGQTSDLTLVTKCANKLENVFDIYEQRLSKSKYLAGEFFSLADLSHLPSLRFLMNEG 180
Arabidopsis thaliana     (AB005238) 121  KPRLGEKCDVVLVEDLKVKLGVVLDIYNNRLSSNRFLAGEEFTMADLTHMPAMGYLMSIT 180
Glycine max              (AF243377) 115  APLTGAPSDQKVIEESDKKIEKVLDVYEERLSKSKYLAGDFFSLADLSHLPFGHYLVNQT 174
Phaseolus acutifolius    (AY099257) 120  ASLFGITPDPKVIEESEAKLLKVLDVYEDRLSKGKYLGGDFLSLADISHLPFIDYIVNKM 179
                                           *   *         *   *   *  ***    * *     **  * *

Citrus sinensis          (DQ198153) 181  GMAHLVTQRKHVNAWWDKISSRPAWKKLASLAH------------------- 213
Vitis vinifera           (AY971515) 181  GMAHLVTERKSVSAWWEDISNRAAWKKVMELAA------------------- 213
Petunia x hybrida        (Y07721)   181  GFSHLVTKRKCLHEWYLDISSRDSWKKVLDLMMKKISEIEAVSIPAKEEAKV 232
Arabidopsis thaliana     (AB005238) 181  DINQMVKARGSFNRWWEEISDRPSWKKLMVLAGH------------------ 214
Glycine max              (AF243377) 175  GRGNLVRDRKHVSAWWDDISNRPAWQKVLQLYKYPV---------------- 210
Phaseolus acutifolius    (AY099257) 180  NKGYLIKERKHVSDWWDDISSRPSWKKVNQLYPPPV---------------- 215
                                                 *     *   ** *  * *   *
```

Figure 1. Alignment of the deduced amino acid sequences of *C. sinensis GST*. Asterisks indicate identical amino acids in all sequences. The analysis of the *GST* protein sequence of orange fruits in the Conserved Domains database revealed the presence of both N-terminal (bold line) and C-terminal (dashed line) conserved domains, which were previously supposed to include the glutathione binding domain and the cosubstrate binding domain, respectively.

Table 1. Analysis of the Expression of *GST* in Different Cultivars of Sweet Orange (*Citrus sinensis* L.) by Real-Time PCR[a]

cultivar	C_T *GST*	C_T *EF*	ΔC_T	$\Delta\Delta C_T$	normalized *GST* amount relative to Navel $2^{-\Delta\Delta C_T}$
Tarocco	25.81 ± 0.006	22.81 ± 0.020	3 ± 0.021	–7.13 ± 0.050	140.78 ± 4.78
Navel	32.95 ± 0.020	22.82 ± 0.010	10.13 ± 0.03	0	1
Ovale	31.56 ± 0.030	22.2 ± 0.050	9.36 ± 0.08	–0.77 ± 0.010	1.71 ± 0.130

[a] The relative quantitation of *GST* expression was calculated using the comparative threshold (C_T) method. For further details, see Materials and Methods.

clone), DQ198153 (Tarocco *GST* complete cds), and AY498567 (*EF-1*α partial coding sequence).

3. RESULTS

3.1. Sequence Analysis of *GST* DNA and cDNA Clones and of Encoded Proteins. The cDNA nucleotide sequence contained a 642 bp open reading frame that encodes a protein of 213 amino acid residues, corresponding to a molecular mass of 24 238.94 Da, with a theoretical pI of 6.39. Sequence analysis and comparison with sequences in the databank revealed high identity of the deduced amino acid sequence with other previously isolated higher plant *GST*s (**Figure 1**). The higher values for identity and similarity were obtained with *GST*s from *Vitis vinifera* (77 and 89%), *Petunia hybrida* (67 and 81%), *Arabidopsis thaliana* (60 and 75%), *Glycine max* (59 and 75%), and *Phaseolus acutifolius* (54 and 72%). The analysis of the *GST* protein sequence of orange fruits in the Conserved Domains database revealed the presence of both N-terminal and C-terminal conserved domains that were previously supposed to include the glutathione binding domain and the cosubstrate binding domain, respectively (*26*). By comparing the red orange *GST* genomic sequence with that of cDNA, three exons of 147, 47, and 446 bp were identified and separated by two introns of 271 and 96 bp, respectively (data not shown). The number and the positions of the two introns match those of all other phi type *GST* genes (*10*). The cDNA as well as the genomic sequences of *GST* were also isolated from non-red orange fruits, both of them being 100% homologous compared to the *GST* clones of pigmented red orange (data not shown).

3.2. Analysis of *GST* Expression in Red and Non-Red Orange Fruits. The expression profile of *GST* was investigated in blood and blond oranges using real-time PCR. The results are shown in **Table 1**, which reports the relative transcript levels of *GST* standardized to the constitutive elongation factor (*EF*) gene expression level and normalized to the Navel $2^{-\Delta\Delta C_T}$. The expression of Tarocco orange *GST* was more than 140 times higher than that measured in the nonpigmented Navel and Ovale orange cultivars, thus suggesting that the phenotypic change from blood to blond might be strictly correlated to the impaired expression of this enzyme. It is worthwhile noting that *EF-1*α partial cDNA clone was amplified every time in all the studied cultivar types with no significant difference in the C_T values, thus demonstrating that the mRNA samples were intact and that the strong decrease in *GST* expression we observed in non-red orange cultivars did not reflect a general decline in mRNA production.

3.3. Measurement of *GST* Activity in the Crude Extract of Orange Fruit. As shown in **Table 2**, the extract of blood orange fruit showed considerable *GST* activity against the artificial substrates NPE and CDNB, the latter being the favorite

Table 2. *GST* Activity of Pigmented (Tarocco) Orange Fruits[a]

substrate	specific activity (nmol/min/mg)
CDNB (1 mM)	220 ± 0.20
NPE (1 mM)	37 ± 0.015
C-3-G (1 mM)	23 ± 0.011

[a] Enzyme activity was carried out on crude extracts (10–30 μg) of orange fruits in a reaction mixture containing 0.1 M phosphate buffer pH 6.8, 1 mM *GSH*, and 1 mM substrates (C-3-G, CNBD, or NPE) and incubation at 30 C° for 15 min. Then, the concentration of the remaining free thiol group of nonconjugated *GSH* was measured adding 2 mL of 5 mM of the Ellman reagent. The absorbance at 412 nm was registered immediately after the addition of the reagent.

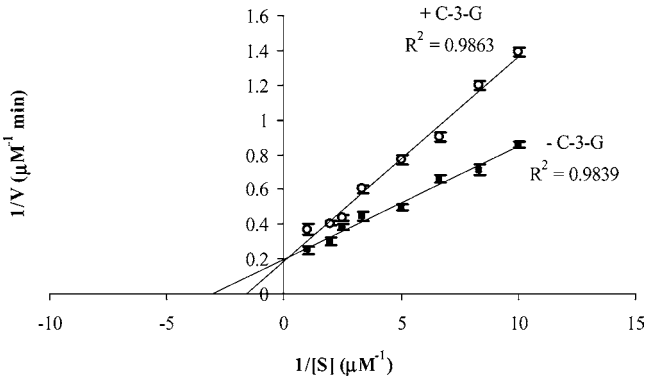

Figure 2. Lineweaver–Burk plots showing the inhibition pattern of C-3-G upon blood orange *GST* activities. The steady-state analysis was carried out as described both in the caption to **Table 2** and in Materials and Methods. Regression lines were drawn for the mean of three experiments.

Table 3. Steady-State Kinetic Parameters of Pigmented (Tarocco) Orange Fruit *GST*[a]

	pigmented orange fruit extracts	
	– C-3-G	+ C-3-G
K_m (mM)	0.33 ± 0.012	0.63 ± 0.011
*V*max (m/min)	5.08 ± 0.15	5.32 ± 0.17
K_{cat}/K_m ($mM^{-1}\,min^{-1}$)	9.86 ± 0.2	5.41 ± 0.11

[a] Steady-state analysis was performed in a reaction medium containing enzyme extract (10–30 μg), 1X PBS pH 7.4 in the presence of 1.5 mM *GSH*, and varying CDNB concentrations in the range of 0.05–1.5 mM. GS-DNB conjugates were detected by measuring the absorbance of samples at 340 nm. To test the effect of C-3-G upon enzyme apparent kinetic parameters, initial velocities were contextually measured in the presence of 80 μM C-3-G.

Table 4. Determination of the Functional Identity of the Cloned *GST* cDNAs[a]

substrate	activity (nmol/min)
1-chloro-2,4-dinitrobenzene (5 mM)	40.5 ± 0.21
cyanidin-3-*O*-glucoside (5 mM)	0.8 ± 0.02

[a] To determine the functional identify of the cloned genes, the *GST* cDNA was subcloned into pEXP1-DEST, which was transcribed and translated in vitro. Subsequently, aliquots of the enzyme extract (10–30 μg) were assayed for *GST* activity by measuring the remaining free thiol group of nonconjugated *GSH*, as described in Materials and Methods.

substrate of the enzyme. *GST* activity was also reproducibly detected when we measured the enzymatic activity providing cyanidin-3-*O*-glucoside (C-3-G) as a substrate (see Materials and Methods for experimental details). Furthermore, we investigated the effect of C-3-G on the *GST* activity of blood orange crude extracts when CBND was the substrate for the enzymes. Increasing concentrations of C-3-G affected the pigmented

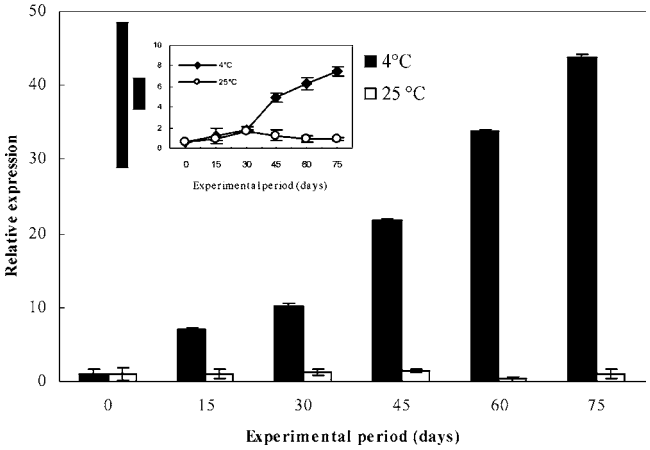

Figure 3. Expression pattern of *GST* in orange juice vesicles during low-temperature exposure. The relative quantitation of gene expression between sample oranges was calculated by real-time PCR using the comparative threshold (C_T) method, as described in the Materials and Methods. Each point represents the mean value of three replications ± SE (or SD). Each replication was composed of six fruits.

orange *GST* activities; at 160 μM C-3-G, the percentage of inhibition was very high (100%) (data not shown). The inhibitory mechanism of C-3-G was determined by steady-state analysis using C-3-G at the concentration required for half-maximal inhibition (**Figure 2** and **Table 3**). As shown in **Table 3**, the apparent K_m value relative to blood orange *GST* was severely increased by the presence of 80 μM C-3-G, whereas no effect was registered upon the V_{max} value; as expected, the catalytic efficiency of blood orange *GST* was also impaired, and so all these data suggest that C-3-G acted as a powerful competitive inhibitor of CDNB conjugation to GSH, as also shown in **Figure 2**.

3.4. Determination of the Functional Identity of the Cloned *GST* cDNAs. To determine the functional identity of the cloned genes, the *GST* cDNA was first subcloned into pEXP1-DEST, resulting in the construct *GST*-pEXP1-DEST, which was transcribed and translated in vitro. Subsequently, aliquots of the enzyme extract (10−30 μg) were incubated in a reaction medium containing either CDNB or CDNB in the presence of GSH to test its ability to conjugate GSH with those different substrates. Interestingly, as shown in **Table 4**, the recombinant protein exhibits *GST* activity against all the substrates, CDNB being the substrate more easily conjugated to GSH. It is also worth pointing out that the *GST* protein produced in vitro was active also in reproducibly conjugating GSH to C-3-G, although it showed a sharply lower value of activity (**Table 4**). Therefore, this finding indicated that the recombinant *C. sinensis* protein is a functionally active *GST* that might be involved in the vacuolar import of anthocyanins in vivo. It has to be emphasized that, as expected, negative control samples carried out with extracts containing empty plasmids as DNA template did not show any *GST* activity.

3.5. Expression Pattern of the *GST* and Anthocyanin Content in Orange Fruits Subjected to Cold Storage. The effect of low-temperature storage upon the anthocyanin content of orange fruits was described in Lo Piero et al. (*21*). Briefly, as reported in the small box within **Figure 3**, the amount of anthocyanins in fruits exposed to low temperatures dramatically increased throughout the entire period. Pigment levels, in fact, rose from an initial value of 0.59 mg/100 g (time zero) to 7.46 mg/100 g (after 75 days storage). On the contrary, in samples kept at 25 °C, the anthocyanin levels increased slightly during

the first 30 days of storage and then decreased, showing values close to the time zero samples. Along with the anthocyanin content, the expression profile of *GST* was also investigated in orange fruits exposed to different storage temperatures using the real-time PCR. The results are illustrated in **Figure 3**, which reports the relative transcript levels of the considered gene standardized to the constitutive *EF-1*α gene expression level and normalized to the time 0 $2^{-\Delta\Delta C_T}$ (see Materials and Methods for details). *GST* was expressed rather constantly along the entire experimental period during the storage at 25 °C. Conversely, after the first 15 days of low-temperature exposure, the levels of transcripts of *GST* began to sharply increase, reaching the maximum values (54-fold respect to time zero) after 75 days of storage. It has to be emphasized that the *EF-1*α partial cDNA clone was amplified in all studied samples with no significant difference in the C_T values between the control and the cold exposed samples, thus demonstrating that the high increase of gene expression observed in the cold stored orange fruits did not reflect a general enhancement in RNA production due to low temperature. Moreover, a negative control represented by RNA samples in which reverse transcriptase was omitted always showed negative C_T.

4. DISCUSSION AND CONCLUSIONS

*GST*s are typically encoded by large gene families, and based on amino acids sequence similarity and gene organization, they are divided into four classes, namely, phi, zeta, tau, and theta. While the two smaller zeta and theta classes have related homologous in animals, the two larger phi and tau *GST*s have been reported only in plants to date (*26*). *GST*s belonging to the phi type share well-defined features as they are encoded by three exon containing genes whose expression was found to be the most highly inducible by diverse stress treatments as compared to that of other *GST* classes (*27*).

In this study, we isolated the genomic clone, as well as the cDNA of the *GST* gene probably involved in the vacuolar import of anthocyanins from orange fruits. A search of the SWISS-PROT database showed that the orange fruit *GST* protein is homologous to the phi class *GST*s since it showed high similarity with other available phi type *GST* sequences, particularly with *AN9* from petunia. Furthermore, the number and the positions of the two introns match those of all other phi type *GST* genes (*10*). As shown in **Figure 1**, there is at least one conserved region in all the aligned *GST* sequences located at the N-terminal half of the protein that probably contains universal traits of *GST*s such as their recognition of *GSH* or their ability to dimerize (*10*). The analysis of available crystal structures of different gluthathione transferases from both animal and plant sources supported this hypothesis (*28*, *29*). A large cavity in the C-terminal half of the *Arabidopsis GST* is proposed as the substrate recognition domain (*29*). By comparing the amino acid sequences of *AN9*, *BZ2*, and the orange fruits' *GST* C-terminal region, we did not find any similar motifs that might represent the substrate binding site (data not shown). In this respect, it has been shown that divergent cytochrome P450 monoxygenase existing in the phenylpropanoid pathway and involved in the synthesis of lignins, flavonoids, and anthocyanins showed highly conserved structural cores and several loop regions despite exhibiting extensive primary sequence diversity (identity as low as 13%). However, those divergent enzymes employ a common strategy to identify their substrates by sharing similar active site architecture (*30*). Similarly, GTSs involved in the vacuolar import of anthocyanins, such as *AN9*, *BZ2*, and orange fruit *GST*s might recognize these pigments through common structural motifs rather than through similar amino acid residues that might constitute the substrate binding site. As expected, the expression level of the *GST* gene in the red and non-red orange cultivars was sharply different, being about 140-fold less in the non-red orange cultivar than in the red one (**Table 1**).

The enzyme from red orange extracts catalyzes the conjugation of *GSH* to either CBND or NPE or C-3-G (**Table 2**), and whenever we tested whether the C-3-G was an inhibitor of the CDNB conjugating activity of the enzymes, we interestingly found that 160 μM C-3-G knocked out the red orange *GST* activity (data not shown). The analysis of the mechanism of this inhibition revealed that C-3-G is a competitive, strong inhibitor of the blood orange *GST* activity, suggesting that this molecule might easily bind the active site of the enzyme and functions as putative substrate (**Figure 2** and **Table 3**).

Our previous results showed that low temperatures induced anthocyanin accumulation in orange fruits (*21*) (box within **Figure 3**). Concordantly, we also found that the expression of crucial structural genes belonging to the anthocyanin biosynthetic pathway such as *PAL*, *CHS*, *DFR*, and *UFGT* was dramatically enhanced by cold treatment. Similarly, we reported here that the expression of the red orange *GST* is strongly induced by cold temperature and that the increase in mRNA production was strictly correlated to that observed for the other structural genes tested, thus confirming that they all have to be considered *cor* (cold regulated) genes (**Figure 3**).

Finally, here we report the successful in vitro translation of orange *GST* cDNAs leading to an active *GST* enzyme that catalyzes the conjugation of *GSH* to the universal substrate CDNB. The recombinant enzyme also conjugates *GSH* to C-3-G (**Table 4**), confirming the involvement of the isolated genes in *GSH*-tagging of anthocyanins, which is the prerequisite for the subsequent vacuolar import. Therefore, our work has laid down the basis for future biochemical analyses to assess the amino acid residues implicated both in substrate binding and in catalysis by using differently site-directed mutated proteins.

ABBREVIATIONS USED

CDNB, 1-chloro-2,4-dinitrobenzene; NPE, nitrophenethyl bromide; C-3-G, cyanidin-3-*O*-glucoside; FAM, 6-carboxyfluorescein; TAMRA, tetramethylrhodamin.

ACKNOWLEDGMENT

Thanks are due to Prof. Antonino Catara and Dr. Vittoria Catara, DISTEF, University of Catania, for providing access to the real-time PCR machine.

LITERATURE CITED

(1) Marrs, K. A. The functions and regulation of glutathione *S*-transferases in plants. *Annu. Rev. Plant Physiol. Plant Mol. Biol.* **1996**, *47*, 127−158.

(2) Sandermann, H., Jr. Plant metabolism of xenobiotics. *Trends Biochem. Sci.* **1992**, *17*, 82−84.

(3) Martinoia, E.; Grill, E.; Tommasini, R.; Kreuz, K.; Amrhein, N. ATP-dependent glutathione *S* conjugates export pump in the vacuolar membrane of plants. *Nature* **1993**, *364*, 247−249.

(4) Lu, Y. P.; Li, Z. S.; Rea, P. A. *At*MRP1gene of *Arabidopsis* encodes a glutathione *S*-conjugates pump: Isolation and functional definition of a plant ATP binding cassette transporter gene. *Proc. Natl. Acad. Sci. U.S.A.* **1997**, *94*, 8243−8248.

(5) Rea, P. A.; Li, Z. S.; Lu, Y. P.; Drozdowicz, Y. M.; Martinoia, E. From vacuolar GS-X pumps to multispecific ABC transportes. *Annu. Rev. Plant Physiol. Plant Mol. Biol.* **1998**, *49*, 727−760.

(6) Goodman, C. D.; Casati, P.; Walbot, V. A multidrug resistance-associated protein involved in anthocyanin transport in *Zea mays*. *Plant Cell* **2004**, *16*, 1812−1826.
(7) Xu, W.; Shioiri, H.; Kojima, M.; Nozue, M. Primary structure and expression of a 24 kD vacuolar protein (VP24) precursor in anthocyanin-producing cells of sweet potato in suspension culture. *Plant Physiol.* **2001**, *125*, 447−455.
(8) Marrs, K. A.; Alfenito, M. R.; Lloyd, A. M.; Walbot, V. A glutathione *S*-transferase involved in vacuolar transfer encoded by the maize gene *bronze2*. *Nature* **1995**, *375*, 397−400.
(9) Coe, E. H.; Hoisington, D. A.; Neuffer, M. G. The genetics of corn. In *Corn and Corn Improvement*; Sprague, G. F., Dudley, J., Eds.; American Society of Agronomy: Madison, WI, 1988; pp 81−258.
(10) Alfenito, M.; Souer, E.; Goodman, C. D.; Buell, R.; Mol, J.; Koes, R.; Walbot, V. Functional complementation of anthocyanin sequestration in the vacuole by widely divergent glutathione *S*-transferase. *Plant Cell* **1998**, *10*, 1135−1149.
(11) Kitamura, S.; Shikazono, N.; Tanaka, A. Trasparent testa 19 is involved in the accumulation of both anthocyanins and proanthocyanidins in *Arabidopsis*. *Plant J.* **2004**, *37*, 104−114.
(12) Mueller, L. A.; Goodman, C. D.; Silady, R. A.; Walbot, V. AN9, a petunia glutathione *S*-transferase required for anthocyanin sequestration, is a flavonoid binding protein. *Plant Physiol.* **2000**, *123*, 1561−1570.
(13) Li, Z. S.; Alfenito, M.; Rea, P. A.; Walbot, V.; Dixon, R. A. Vacuolar uptake of the phytoalexin medicarpin by the glutathione conjugate pump. *Phytochemistry* **1997**, *45*, 689−693.
(14) Rapisarda, P.; Giuffrida, A. Anthocyanin level in Italian blood oranges. *Proc. Int. Soc. Citric.* **1992**, *3*, 1130−1133.
(15) Maccarone, E.; Rapisarda, P.; Fanella, F.; Arena, E.; Mondello, L. Cyanidin-3-(6″-malonyl)-β-glucoside. One of the major anthocyanins in blood orange juice. *Ital. J. Food Sci.* **1998**, *10*, 367−372.
(16) Amorini, A. M.; Lazzarino, G.; Galvano, F.; Tazzina, G.; Gavazzi, B.; Galvano, G. Cyanidin-3-*O*-β-glucopyranoside protects myocardium and erythrocytes from oxygen radical-mediated damages. *Free Radical Res.* **2003**, *37*, 453−460.
(17) Lo Piero, A. R.; Puglisi, I.; Consoli, A.; La Rosa, M.; Reforgiato Recupero, G.; Petrone, G. Cloning and sequencing of structural genes involved in anthocyanin biosynthesis in blood orange. *Proc. XLV Ital. Soc. Agric. Genet.* **2001**, *1*, 5.58.
(18) Lo Piero, A. R.; Consoli, A.; Puglisi, I.; Orestano, G.; Reforgiato Recupero, G.; Petrone, G. Anthocyaninless cultivar of sweet orange lacks expressions of the UDP-glucose flavonoid 3-*O*-glucosyl transferase. *J. Plant Biochem. Biotechnol.* **2005**, *14*, 1−6.
(19) Lo Piero, A. R.; Puglisi, I.; Petrone, G. Gene characterization, analysis of expression, and in vitro synthesis of dihydroflavonol 4-reductase from [*Citrus sinensis* (L.) *Osbeck*]. *Phytochemistry* **2006**, *67*, 684−695.
(20) Cotroneo, P. S.; Lo Piero A. R.; Ciuni, M.; Consoli, A.; Puglisi, I.; Morana, L.; Russo, M. P.; Reforgiato Recupero, G.; Petrone, G. Cloning, sequencing and expression levels of several genes involved in the anthocyanin biosynthesis pathway in *Citrus* genus. *Proc. XLV Ital. Soc. Agric. Genet.* **2002**, *1*, S1e.
(21) Lo Piero, A. R.; Puglisi, I.; Rapisarda, P.; Petrone, G. Anthocyanin accumulation and related gene expression in red orange fruit induced by low-temperature storage. *J. Agric. Food Chem.* **2005**, *53*, 9083−9088.
(22) Heid, C.; Stevens, J.; Livak, K.; Williams, P. Real-time quantitative PCR. In *Genome Methods: Genome Research*; Cold Spring Harbor Laboratory Press: Plainview, NY, 1996.
(23) Mahe, A.; Grisvard, J.; Dron, M. Fungal and plant specific gene markers to follow the bean anthracnose infection process and normalize a bean chitinase mRNA induction. *Mol. Plant-Microbe Interact.* **1992**, *5*, 242−248.
(24) Bradford, M. M. A rapid and sensitive method for the quantitation of microgram quantities of protein utilizing the principle of protein−dye binding. *Anal. Biochem.* **1976**, *72*, 248−254.
(25) Holt, D. C.; Lay, V. J.; Clarke, E. D.; Dinsmore, A.; Jepson, I.; Bright, S. W. J.; Greenland, A. J. Characterization of safener-induced glutathione *S*-transferase isoform II from maize. *Planta* **1995**, *196*, 295−302.
(26) Edwards, R.; Dixon, D. P.; Walbot, V. Plant glutathione transferases: enzymes with multiple functions in sickness and in health. *Trends Plant Sci.* **2000**, *5*,193−198.
(27) Wagner, U.; Edwards, R.; Dixon, D. P.; Mauch, F. Probing the diversity of the *Arabidopsis* glutathione *S*-transferase gene family. *Plant Mol. Biol.* **2002**, *49*, 515−532.
(28) Pemble, S. E.; Taylor, J. B. An evolutionary perspective on glutathione transferases inferred from class theta glutathione transferase cDNA sequences. *Biochem. J.* **1992**, *287*, 957−963.
(29) Reinemer, P.; Prade, L.; Hof, P.; Neuefeind, T.; Huber, R.; Zetti, R.; Palme, K.; Schell, J.; Keolin, I.; Bartunik, H. D.; Bieseler, B. Three-dimensional structure of glutathione *S*-transferase from *Arabidopsis thaliana* at 2.2 Å resolution: Structural characterization of herbicide-conjugating plant glutathione *S*-transferases and a novel active site architecture. *J. Mol. Biol.* **1996**, *255*, 289−309.
(30) Rupasinghe, S.; Baudry, J.; Schuler, M. A. Common active site architecture and binding strategy of four phenylpropanoid P450s from *Arabidopsis thaliana* as revealed by molecular modeling. *Protein Eng.* **2003**, *16*, 721−731.

Received for review June 15, 2006. Revised manuscript received September 7, 2006. Accepted September 20, 2006. Financial support was provided by the MIPAF research project "Ricerche e sperimentazioni nel settore dell'agrumicoltura Italiana" and by "Progetti di Ricerca di Ateneo−Fondi del bilancio universitario: Effetto della conservazione a due diverse temperature sulla biosintesi delle antocianine in polpa di arance rosse", University of Catania, 2004.

JF0616816